Reconstitution of Transferrin Receptor in Mixed Lipid Vesicles. An Example of the Role of Elastic and Electrostatic Forces for Protein/Lipid Assembly†

A. Kurrle,‡ P. Rieber,§ and E. Sackmann*,‡

Physik Department, Biophysics Laboratory E22, Technische Universität München, James-Franck-Strasse, 8046 Garching, Germany, and Institut für Immunologie, Ludwig Maximilians Universität, Goethestrasse 31, 8000 München 2, Germany

Received January 5, 1990; Revised Manuscript Received May 24, 1990

ABSTRACT: We studied the interaction of transferrin receptors (of cell line Molt-4) with mixed model membranes as a function of lipid chain length (phospholipids with C14:0 and C18:1 hydrocarbon chains) and of the surface charge of the membrane using mixtures of C14:0 lecithin (DMPC) with C14:0 phosphatidylglycerol (DMPG) and C14:0 phosphatidylserine (DMPS). Spontaneous self-assembly of receptors and lipids was achieved by freeze–thaw cycles of a codispersion of mixed vesicles and receptors in buffer and subsequent separation of receptor-loaded and receptor-free vesicles by density gradient centrifugation. Information on specific lipid/protein interaction mechanisms was obtained by evaluation of protein-induced shifts of phase boundaries of lipid mixtures by calorimetry and by FTIR spectroscopy of partially deuterated lipid mixtures. The important role (1) of minimizing the elastic forces caused by the mismatch of the lengths of hydrophobic cores of the protein (l_p) and the bilayer (l_L) and (2) of the electrostatic coupling of protein head groups with the charged membrane/water interface for the lipid/protein self-assembly is established. The electrostatic interaction energy per receptor is about 10^3 k_BT (by coupling to about 1000 charged lipids) which is sufficient to overcompensate the elastic energy associated with a mismatch of $l_p - l_L \approx 1.0$ nm. The maximum receptor concentration incorporated was measured as a function of membrane surface charge and lipid chain length. The maximum receptor molar fraction varied from $x_p^{max} = 5 \times 10^{-5}$ for DMPC to $x_p^{max} = 4 \times 10^{-4}$ for 1:1 DMPC/DMPG; moreover x_p^{max} is higher for DMPS than for DMPG as charged component. For the long-chain lipids, x_p^{max} is higher for a 9:1 DEPE/DEPC mixture [$(4.2–9) \times 10^{-4}$] than for pure DEPC (ca. 3.5×10^{-4}). By decomposition of reconstituted receptors with proteases, we demonstrated the homogeneous orientation of the receptor with its extracellular head group pointing to the convex side of the vesicles. Finally, binding curves of FITC-labeled Fe–transferrin to reconstituted receptors were recorded. The dissociation constant (about $K_D \approx 10^{-8}$ M) is reduced in bilayers with unmatched thickness, pointing to elastic distortion of the receptor. The binding curves of the (acidic) ligand to the charged membranes exhibit sigmoidal shape owing to electrostatic repulsion causing a ligand depletion zone on the membrane surface.

The transferrin receptor is a transmembrane protein which mediates the transfer of iron into cells via the serum protein transferrin. It belongs to the class of receptors (such as the insulin receptor) which (together with their ligands) are internalized by endocytosis after accumulation in coated pits. However, in contrast to the case of the insulin receptor, the binding of the ligand transferrin is not associated with a marked conformational change of the receptor or phosphorylation of the cytoplasmic domain, and the transferrin molecule is recycled together with the receptor.

One motivation for the present and previous work on insulin receptor (Sui et al., 1988) was to develop procedures for the incorporation of receptors into synthetic lipid bilayer vesicles in a well-defined manner for future studies on the effect of ligand binding on the receptor conformation and/or the interaction of the cytoplasmic domain with elements of the cytoplasmic network. Moreover, it was shown previously (Sui et al., 1988) that planar lipid/receptor bilayers may be deposited onto glass substrates by fusion of the reconstituted vesicles on the glass surface. Such supported bilayers are well suited to measure binding constants of ligands, agonists, or antagonists to the receptors and their modulation by the lipid composition. It is hoped that such measurements become helpful for future drug design in order to predict side effects of newly synthesized drugs.

Moreover, the present work is a continuation of our previous efforts (Maksymiw et al., 1987; Sui et al., 1988) to evaluate physical mechanisms of selective lipid/protein interaction. The above-mentioned as well as other studies (Jähnig, 1978; Sperotto & Mouritsen, 1988) provided strong evidence that both the interaction of the membrane-spanning part of the protein with that of the lipid bilayer and also the interaction of the protein head group with the bilayer surface play an essential role for the preference of certain lipids by the protein. In the former case, the selectivity is mediated by the elastic deformation of the lipid bilayer by the protein (Mouritsen & Bloom, 1984; Sackmann, 1984; Riegler & Möhwald, 1986) while in the latter case electrostatic forces (Maksymiw et al., 1987), hydrogen bonds, and physisorption of the protein head group to the bilayer surface (Rüppel et al., 1982) may come into play. In order to explore the contribution of the two mechanisms, we reconstituted the transferrin receptor (TFR)[1] in lecithin vesicles of different chain length and in mixtures of lecithin and ethanolamine and of lecithin with charged

† Supported by the Deutsche Forschungsgemeinschaft (Sa 246/19-2), the Fonds der Chemischen Industrie, and the Freunde der TUM.

* Address correspondence to this author.
‡ Technische Universität München.
§ Ludwig Maximilians Universität.

[1] Abbreviations: FTIR, Fourier transform infrared spectroscopy; TFR, transferrin receptor; DMPC, dimyristoylphosphatidylcholine; DMPG, dimyristoylphosphatidylglycerol; DMPS, dimyristoylphosphatidylserine; DEPE, dielaidoylphosphatidylethanolamine; DEPC, dielaidoylphosphatidylcholine; FITC, fluorescein isothiocyanate.

0006-2960/90/0429-8274$02.50/0

lipids. Reconstitution is achieved by the freeze–thaw technique and the separation of loaded and unloaded vesicles by density gradient centrifugation. The lipid/protein interaction is studied (1) by calorimetry which provides quantitative information on the lipid/protein interaction energy and (2) by FTIR[1] which (in combination with partial deuteration) allows differentiation between the interaction of the protein with the head group and the hydrocarbon chains of the different lipids. Various biochemical and fluorescence spectroscopic methods were applied in order (1) to determine the protein to lipid ratio in the reconstituted vesicles, (2) to obtain information on the orientation of the receptor in the vesicle, and (3) to evaluate the binding of transferrin to the reconstituted vesicles as a function of lipid composition.

Materials and Methods

Materials. DMPC was obtained from Fluka. DMPG, DMPS, DEPC, and chain-deuterated DMPC were purchased from Avanti Polar Lipids. DEPE was kindly provided by Dr. W. Knoll (Universität Mainz). The detergent Nonidet-P40 (NP-40) was from Sigma and deoxycholic acid sodium salt (NaDOC) from Serva. Metrizamide was purchased from Serva. Transferrin was obtained from Calbiochem.

Cell Culture and Preparation of Cell Lysates. A cell line derived from an acute lymphoblastic leukemia, Molt-4 (Minowada et al., 1972), was grown under a 5% CO_2 atmosphere in RPMJ 1640 medium, supplemented with 100 units of penicillin/streptomycin and 5% heat-inactivated fetal calf serum. Cells were harvested by centrifugation when they had reached a density of 5×10^5 cells/mL. After being washed twice with phosphate-buffered saline, they were resuspended in lysis buffer (150 mM NaCl, 10 mM Tris-HCl, pH 8.2, 1 mM EDTA, 2 mM phenylmethanesulfonyl fluoride, 2 mM benzamidine, and 1% NP-40); 5×10^7 cells/mL of lysis buffer were extensively stirred on a Vortex, and after 15 min at 4 °C, the lysate was centrifuged (9000*g* for 60 min). The supernatant was removed and brought to 0.5 M NaCl by the addition of 3.5 M NaCl. The lysate was then used for immune adsorption on the affinity matrix.

Isolation and Purification of Transferrin Receptor by Immunochromatography. This procedure was partially adopted from Schneider et al. (1982) (with some modifications). Freshly prepared cell lysates (typically from about 10^{10} cells) were loaded on an affinity column [Affi-gel 10 with coupled monoclonal antibody 2-17 (IgG) directed against human transferrin receptor]. To elute unspecifically bound material, the column was washed in sequence with the following three buffers: (I) 500 mM NaCl, 50 mM Tris-HCl, pH 8.2, 1 mM EDTA, and 0.5% NP-40; (II) 150 mM NaCl, 50 mM Tris-HCl, pH 8.2, 0.5% NP-40, and 0.1% SDS; (III) 150 mM NaCl and 0.25% NaDOC (two washes).

Transferrin receptors specifically bound to the matrix were eluted from the beads with an equal volume of 50 mM diethylamine, pH 11.5, containing 0.25% NaDOC. The eluted material was immediately brought to near-neutrality (ca. pH 8.0) by the addition of 0.5 M NaH_2PO_4. The beads were washed extensively in borate buffer, pH 8.0, and stored in this buffer. Finally, the eluted transferrin receptor was concentrated to 0.5–1 mg/mL, dialyzed against detergent-free reconstitution buffer (150 mM NaCl, 50 mM Tris-HCl, pH 8.0, 3 mM EDTA, 0.1 mM DTT, and 1 mM NaN_3), and stored at −70 °C.

Reconstitution Procedure. The lipids (typically 3 mg) were dissolved in chloroform or chloroform/methanol (3:1) if the lipid mixture contained DMPS. The organic solvent was evaporated under a stream of nitrogen and totally removed during an overnight incubation in an exsiccator. The dry lipid film was dispersed in reconstitution buffer at a temperature above its gel-to-liquid-crystalline phase transition temperature (T_m) and incubated at this temperature for 1 h. Then the lipid dispersions were sonicated at this temperature using a Branson tip sonifier (5–10 min, 40 W) until the sample appeared clear or slightly opalescent. Then the transferrin receptor was added in the desired quantity, and the suspensions were quickly frozen in liquid nitrogen and slowly thawed. This cycle was repeated 4 times. Finally, the samples were incubated for 15 min above T_m. Control liposomes were prepared in an analogous manner but without addition of the receptor protein.

Separation of Proteoliposomes from Pure Lipid Vesicles and Free Protein. After the reconstitution procedure, vesicle suspensions were mixed with metrizamide to give a solution of 40% metrizamide. This solution was transferred into a centrifuge tube. Then 20% metrizamide in reconstitution buffer was overlayered, followed by another overlay of pure buffer to form a discontinuous density gradient. Centrifugation was carried out at 100000*g* for 2 h at 29 °C. The turbid band containing the lipid/protein complex (proteoliposomes) could be seen distinctly and was clearly separated from pure lipid vesicles. The bands of interest were recovered with a plastic syringe and dialyzed against reconstitution buffer.

Binding Studies. The proteovesicles prepared by the freeze–thaw method were separated from unbound TFR by centrifugation and subsequently dialyzed against the buffer used for the binding studies (50 mM Tris/100 mM NaCl, pH 7.8). The samples were incubated for 1 h at 4 °C with FITC-labeled Fe–transferrin and 1% BSA. The latter was added in order to reduce unspecific binding which was particular strong for PE. Following the procedure of Nunez and Glass (1982), the samples were stored on ice and adjusted to pH 6.5 by adding 0.5 M NaH_2PO_4 in order to stabilize the transferrin binding. Then the nonbound FITC–Fe–transferrin was removed by density gradient centrifugation. The vesicle-containing band was taken up in the buffer, and the fluorescence spectra were taken with a Schoeffel RRS 1000 spectrofluorometer. The samples were filled into microfluorescence cuvettes (Hellma) and stirred continuously. The excitation wavelength was 482 nm, and the emission was measured at 520 nm. For quantitative determination of the bound ligand, the fluorescence intensity was compared with that of a test solution containing defined amounts of FITC–Fe–transferrin and protein-free vesicles, to account for the turbidity of the samples.

Calorimetry. High-sensitivity DSC measurements were performed with an MC-2 microcalorimeter (Microcal, Amherst, MA). The data were stored and analyzed by an IBM AT computer using the DA-2 software provided by Microcal. The samples were transferred to a cooling bath and equilibrated at the starting temperature of the hs-DSC scan for at least 15 min and then filled into the calorimeter. The heating scan was started after additional 10-min equilibration with a scan rate of 30 °C/h (if not stated otherwise) and a 15-s time increment (filter constant) between each data acquisition step. The transition enthalpies (ΔH) were determined by integration after subtraction of the buffer base line. The integration limits were defined by connecting the regions of flat base line with a straight line.

FTIR Measurements. For FTIR measurements, a Nicolet 60 SXB spectrometer equipped with a liquid ATR accessory (thermostated 5-mL cylindrical cell with ZnS crystal from Spectratech) and a MCT detector was used. The temperature was measured at the sample cell using a Pt 100 thermocouple

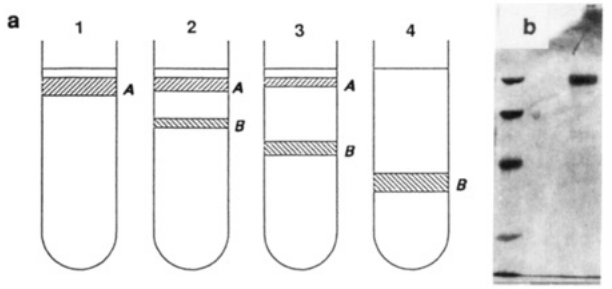

FIGURE 1: Separation of vesicles in a metrizamide density gradient. (a) Schematic view of the distribution of two vesicle populations [A (protein free) and B (protein loaded)] in the density gradient: (1) DMPC/DMPG 1:1 without receptor; (2) TFR in DMPC/DMPG 9:1; (3) TFR in DMPC/DMPG 7:3; (4) TFR in DMPC/DMPG 1:1. Note the absence of band A in the last case. (b) SDS gel of standard proteins and of density fractions of (a). The standard proteins are shown on the left side [from top to bottom, molecular weight ($\times 10^{-3}$): 92.5, 66.2, 45, and 31]. Bands A and B from sample 2 (a) are shown in the center and on the right side, respectively.

which controlled an external water bath and was constant within ±0.2 °C. The measurements were performed from lower to higher temperatures for each sample. At each temperature, 100 scans were accumulated at a resolution of 2 cm^{-1} between 4000 and 400 cm^{-1}. The buffer spectra were recorded separately at the same temperatures and interactively subtracted from the sample spectra. The frequency of the methylene stretching vibrations was determined as the maximum of the corresponding bands.

RESULTS

Density Gradient Separation of Protein-Free and -Loaded Vesicles. Figure 1a shows a schematic view of the distribution of protein-free and protein-loaded vesicles after separation in a metrizamide density gradient by centrifugation. On the left side (sample 1), the case of protein-free vesicles (a 1:1 DMPC/DMPG mixture) is shown. As expected, only one band is observed. Samples 2–4 on the right side of Figure 1a show the cases of reconstituted TRF in DMPC/DMPG mixed vesicles. From sample 2 to 4, the concentration of the charged component increases. Clearly, two separate bands are observed in these cases. The upper one is located at the same position as the protein-free control vesicles while the lower one is shifted to higher densities with increasing content of DMPG. The SDS gel electrophoresis experiments in Figure 1b clearly demonstrate that the heavier fraction B contains the protein. The shift of band 3 to higher densities with increasing DMPG content shows that the fraction of protein incorporated into DMPC/DMPG vesicles increases with increasing surface charge of the membrane. (Note that the initial protein concentration during the freeze–thaw procedure was the same in all samples of Figure 1.)

Calorimetric Studies. In a first series of experiments, we studied the effect of the transferrin receptor (TFR) on the phase transition of pure lipid bilayers and on the phase separation of lipid mixtures. As shown in previous studies (Maksymiw et al., 1987; Sui et al., 1988; Bach, 1984; McElhaney, 1986), such studies provide a valuable tool to quantify the lipid/protein interaction in terms of the excess free energy of lipid/protein interaction: the work required to transfer the protein from a (hypothetical) ideal solution (in a bilayer) into the real solution. In order to explore the structural basis of the selective lipid/protein interaction, we studied the interaction of TFR with bilayers first of different thickness (lipid chains with 14 and 18 C atoms) and second of different surface charge density (by adding growing amounts

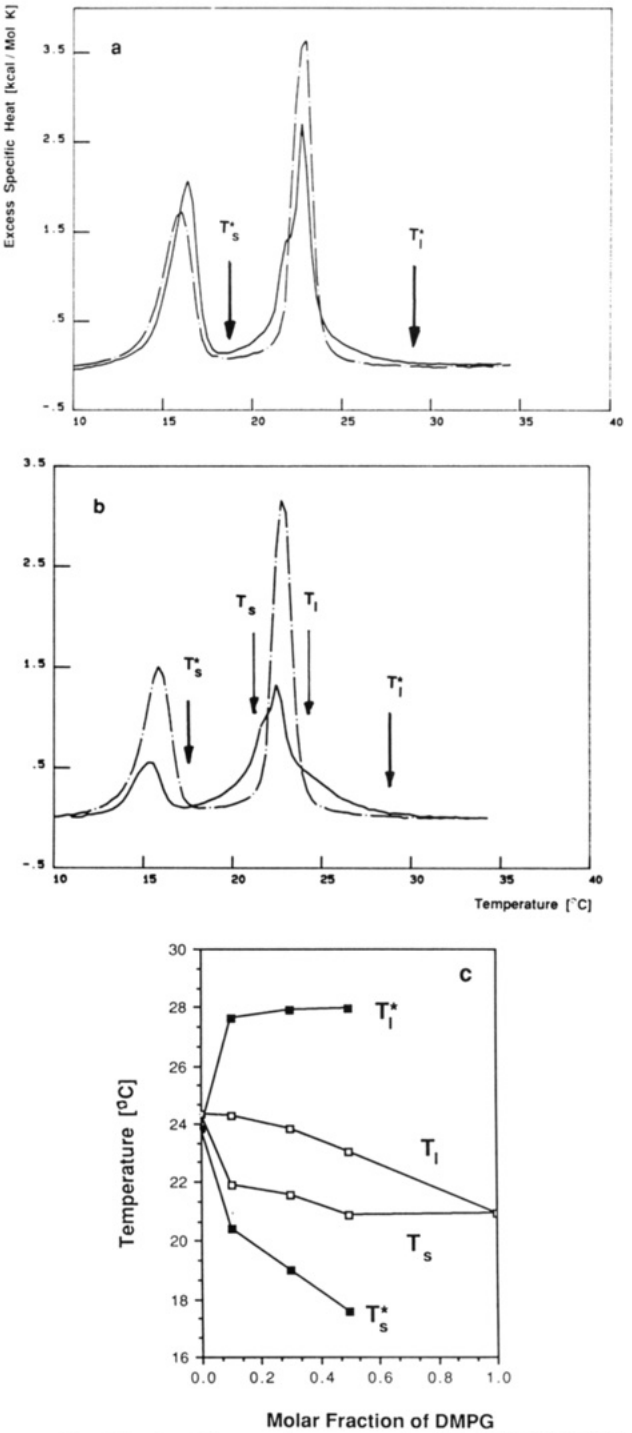

FIGURE 2: Calorimetric scanning curves of a 1:1 DMPC/DMPG mixture without (–·–) and with (—) transferrin receptor. The ordinate gives the specific heat in kilocalories per mole per kelvin. (a) Protein molar fraction with respect to lipid, $x_p = 2.4 \times 10^{-4}$ (corresponding to mass fraction $x_m = 5.4 \times 10^{-2}$); (b) protein molar fraction, $x_p = 3.7 \times 10^{-4}$ ($x_m = 8.3 \times 10^{-2}$); (c) phase diagram of the binary lipid mixture DMPC/DMPG (□) and its modification by the transferrin receptor (■).

of PG and PS). In all cases, the receptor concentration was kept low in order to minimize effects of protein/protein interaction. A few examples of our calorimetric studies are presented in Figures 2–5 together with freeze–fracture electron microscopic observations of the vesicle structure.

DMPC/DMPG and DMPC/DMPS Mixtures. Figure 2a,b shows the effect of two different concentrations of the receptor (molar fraction $x_p = 2.4 \times 10^{-4}$ and $x_p = 3.7 \times 10^{-4}$) on the scanning calorimetric curves of a 1:1 DMPC/DMPG mixture,

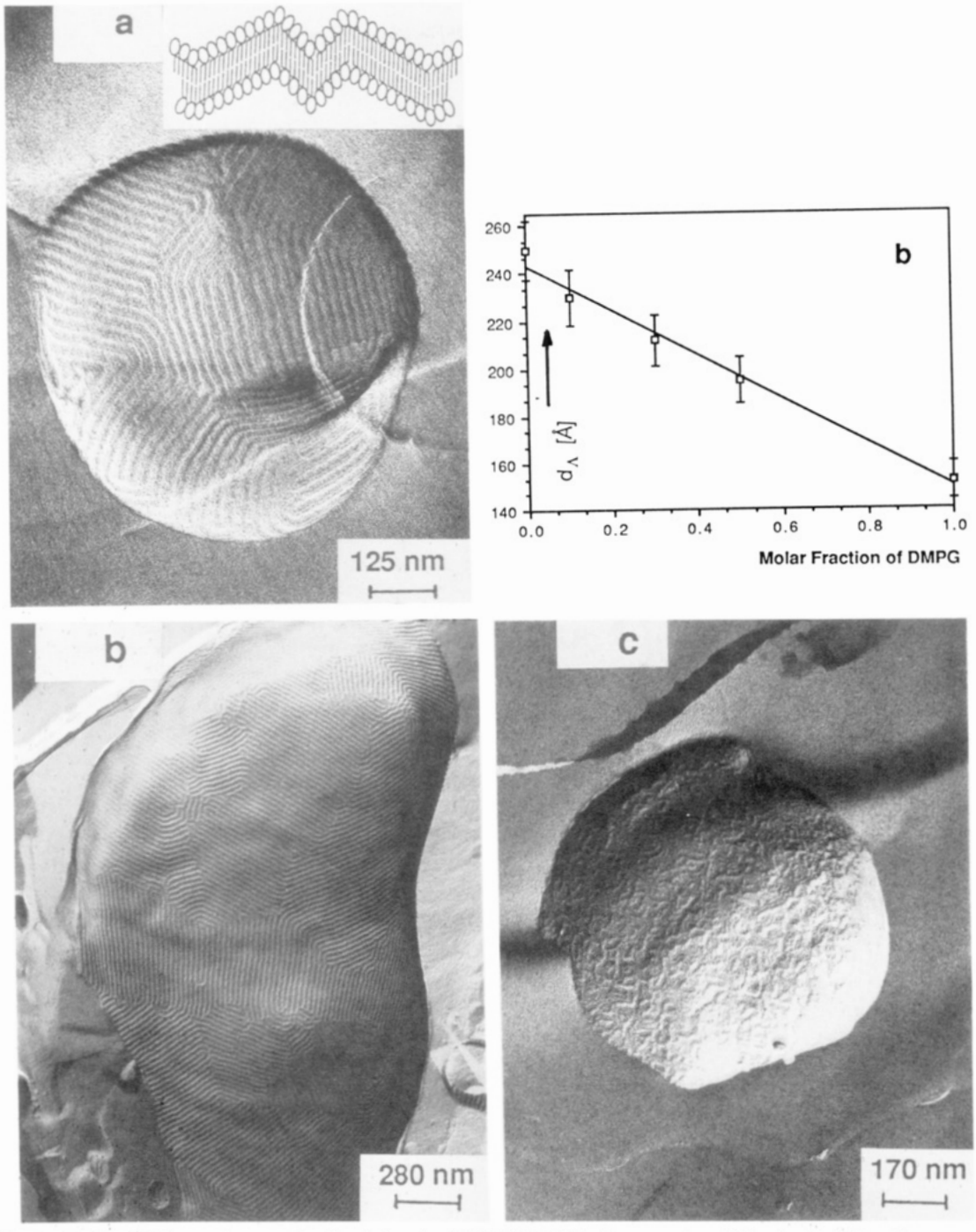

FIGURE 3: Freeze–fracture electron micrographs of vesicles of a DMPC/DMPG mixture and modification by TFR. The preparations were frozen from 17 °C. (a) Ripple phase ($P_{\beta'}$) of equimolar mixture. Note that each ripple exhibits a fine groove in the center and exhibits a profile as indicated in the insert. This corresponds to the Λ conformation (Rüppel & Sackmann, 1983). (b) Plot of ripple repeat distance d_Λ as a function of DMPG concentration. (b) Micrograph of 7:3 DMPC/DMPG mixture containing $x_p = 3.2 \times 10^{-4}$ TFR. Note the absence of groove. (c) Micrograph of a 1:1 mixture containing $x_p = 3.7 \times 10^{-4}$ TFR.

and Figure 2c summarizes the shifts of the liquidus line (from T_l to T_l^*) and of the solidus line (from T_s to T_s^*) of the DMP/DMPG mixture for a protein molar fraction of x_p = 0 to $x_p = 3.7 \times 10^{-4}$.

The pure lipid mixture exhibits a rather sharp cigarlike phase diagram, and a pronounced pretransition is observed for all compositions. This shows that the lipid mixture exhibits ideal behavior and complete miscibility in the fluid and solid state. Evidence for this is also provided by the freeze–fracture electron micrographs of Figure 3. Clearly, the surface profile of the vesicle of the 1:1 mixture exhibits a well-defined ripple texture. The profile of each ripple shows a fine groove in the center (cf. schematic view of Figure 3a), and the ripple phase is thus of the Λ type (Rüppel & Sackmann, 1983). The near-ideality of the DMPC/DMPG mixture is further demonstrated by the finding that the wavelength varies linearly with composition between a value of Λ = 24 nm for pure DMPC to Λ = 15 nm for DMPG.

The transferrin receptor exerts a pronounced effect on the $L_\alpha \rightarrow P_{\beta'}$ transition of the nearly ideal (1:1) DMPC/DMPG mixture: first, the liquidus line is shifted from T_l = 24 °C to $T_l^* \approx 29$ °C. However, the shift does not depend appreciably on the protein molar fraction; that is, only the height of the high-temperature shoulder increases with the protein content. Second, the solidus line is shifted to lower temperatures; however, in this case, the shift $\Delta T = T_s - T_s^*$ increases with

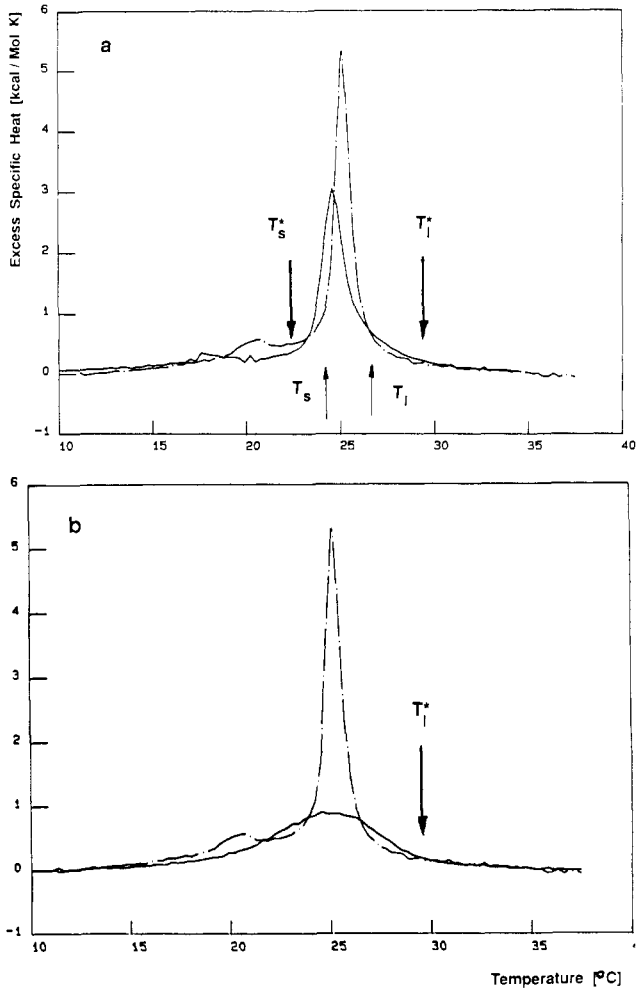

FIGURE 4: Calorimetric scanning curves of an 8:2 mixture of DMPC and DMPS (-·-) and the effect of TFR (—) at two different concentrations: $x_p = 1.5 \times 10^{-4}$ (a); $x_p = 4.7 \times 10^{-4}$ (b). The ordinate gives the specific heat in kilocalories per mole per kelvin. Only T_l^* can be determined with some accuracy.

x_p. The modification of the phase boundary lines of the chain-melting ($L_\alpha \rightarrow P_{\beta'}$) transition is summarized in Figure 2c.

The effect of the TFR on the ripple texture depends on the DMPG content. At low concentration of the charged lipid (<30 mol %) and of the protein, one observes a well-defined ripple texture (cf. Figure 3c); only the central groove vanishes. This provides strong evidence that the ternary lipid/lipid/protein system forms a homogeneous solid solution. At high protein and DMPG content, the texture exhibits completely distorted ripples and smooth domains which points to phase separation.

Figure 4 shows the effect of the receptor on the phase change of an 8:2 DMPC/DMPS mixture for two protein concentrations: $x_p = 1.5 \times 10^{-4}$ and $x_p = 4.7 \times 10^{-4}$. Again, the liquidus line is shifted to high temperatures and the solidus to low temperatures. The shift of the former ($\Delta T = T_l^* - T_l$) is again essentially independent of the protein concentration. The shift of the solidus line increases again with increasing protein content, although the position T_s^* cannot be determined accurately.

The shifts of the solidus and liquidus lines in opposite directions appear to contradict the rule of thermodynamic stability if the mixture can be considered as binary. It can, however, be understood in terms of two separate lipid/protein interaction mechanisms: (1) the electrostatic coupling of the protein head group to the charged lipid component and (2)

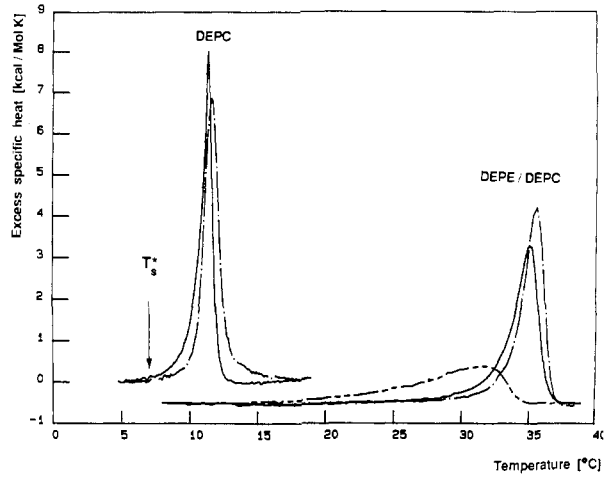

FIGURE 5: Effect of TFR on scanning calorimetric curves of zwitterionic lipid with trans-C 18:1 hydrocarbon chains. Left: Transition of DEPC in the absence (-·-) and presence (—) of $x_p = 3.4 \times 10^{-4}$ TFR. Right: Transition of vesicles of a 9:1 mixture of DEPE/DEPC (-·-) and effect of TFR at molar fractions of $x_p = 4.2 \times 10^{-4}$ (—) and $x_p = 9.1 \times 10^{-4}$ (-·-).

the hydrophobic interaction of the membrane-spanning domains and the fatty acids of the receptor with the hydrophobic core of the membrane.

In Figure 5, examples of the effect of the transferrin receptor on the phase transition curves of vesicles of zwitterionic long-chain lipids are shown, namely, DEPC and DEPE containing 10% DEPC. The latter component was mixed with DEPE to facilitate swelling into bilayer vesicles. In this case, both the liquidus and solidus lines are shifted to low temperatures. This low-temperature shift of T_l and T_s is in agreement with previous reconstitution experiments of the insulin receptor and glycophorin in DMPC vesicles and provides further evidence for the above conclusion that the high-temperature shift of DMPG is caused by electrostatic interaction of the head group with the charged component. It is also noteworthy that the shift of the phase boundaries is slightly, however significantly, larger for DEPC than for DEPE. This suggests a somewhat larger perturbation of the structure of the former lipid by the receptor.

Figures 2, 4, and 5 lead to the following conclusions: The interaction of the hydrophobic domain of the protein with the membrane leads to a shift of the liquidus as well as the solidus lines (which are determined by the onsets and end points of chain melting, respectively) to lower temperatures. The high-temperature shift of the liquidus line observed in the presence of DMPG and DMPS is caused by the electrostatic interaction of the receptor head group with the charged lipid component.

FTIR Spectroscopy. In order to get further insight into the selective lipid/protein interaction mechanisms, FTIR spectra of vesicles with one of the lipid components deuterated were taken in the absence and presence of receptors. As is well-known, FTIR spectroscopy is a powerful technique to study phase transitions of lipid bilayers owing to the pronounced low-frequency shift of the symmetric C-H (or C-D) vibrational bands at the fluid to solid transition. A further advantage of FTIR spectroscopy is that the C-D and C-H bands can be distinguished in the spectra which allows detection of the transition of the deuterated and nondeuterated lipid components separately in mixed membranes.

Figure 6 shows the result for the DMPG/DMPC-d_{54} (chain deuterated only) mixture. The positions of the symmetric C-D vibrations of DMPC-d_{54} and of the C-H vibration of DMPG

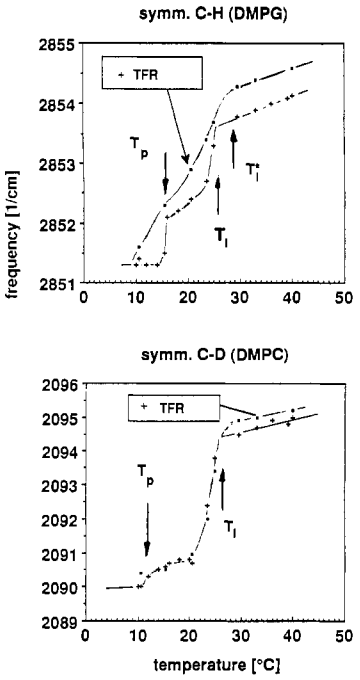

FIGURE 6: FTIR spectra of a vesicle suspension of a 1:1 DMPC-d_{54}/DMPG mixture [curves marked by (+)] and effect of TFR at molar fraction $x_p = 3.7 \times 10^{-4}$ [curves marked by (■)]. Top: Plot of the position of the symmetric C–H vibration of DMPG as a function of temperature. Bottom: Plot of the symmetric C–D vibration of DMPC-d_{54}. Note the clear indication of a pretransition (at temperature T_p) in both cases. The positions of the liquidus line in the absence (T_l) and presence (T_l^*) of TFR are indicated by arrows. The modified solidus line cannot be located.

are recorded as a function of temperature. Consider first the pure lipid mixture. The phase changes about the chain-melting transition and the pretransition are well indicated by abrupt changes in the position of the bands. Interestingly, the latter is much more pronounced for DMPG than for DMPC. Its sharpness provides further evidence for the complete miscibility of the mixture in the $P_{\beta'}$ phase.

Incorporation of the TFR affects the spectrum of DMPG much stronger than that of DMPC. First, above the chain-melting transition ($T > T_l^*$), the relative shift at 35 °C for the former lipid is $\Delta\nu/\nu_0 \approx 5 \times 10^{-4}$ as compared to $\Delta\nu/\nu_0 = 2 \times 10^{-4}$ for the latter, where ν_0 is the frequency of the protein-free sample. Second, the temperature dependence of the C–D spectrum of DMPC-d_{54} agrees closely with that in the absence of TFR, with the exception of the pretransition which is suppressed. For DMPG, however, the frequency is shifted to higher values both above and below the liquidus line in the presence of the receptor. Third, the onset of the phase change (as indicated by the drop in frequency at decreasing temperature) occurs at $T_l^* \approx 29$ °C for DMPG but appears to be much less shifted for DMPC ($T_l^* \approx T_l$). These findings provide clear evidence that the transferrin receptor has a pronounced preference for the charged lipid.

Treatment of Reconstituted Receptor with Pronase. In order to get further information concerning the interaction of the receptor with the lipid bilayer and in order to find out whether the TFR is completely penetrating the bilayer, we treated reconstituted vesicles with Pronase. By use of such a mixture of proteases which decomposes the proteins completely into amino acids, the interpretation of results is facilitated. Figure 7a shows the effect on the phase change of the 1:1 DMPC/DMPG bilayer. Comparison of the two thermograms shows that the high-temperature shift of the liquidus line vanishes completely while the decrease of the solidus line is still clearly visible. This dramatic change of the lipid/protein interaction is also reflected in the freeze–fracture electron micrographs shown in Figure 7b: the texture changes from the Λ type before to the Λ/2 type after treatment with Pronase. Finally, the approximate molecular weight of the residual polypeptide (not decomposed by Pronase) was determined by SDS gel electrophoresis. The result is shown in Figure 7c (lane A). Comparison with the trace of a mixture of standard proteins (lane C) shows that the residual fraction exhibits a molecular weight of 10K. No remarkable traces of other species are observed. The molecular weight corresponds exactly to the hydrophobic domain and the cytoplasmatic head group of the receptor. In summary, Figure 7 leads to the following conclusions:

(1) The high-temperature shift of the liquidus line is caused by the electrostatic interaction of the extracellular head group of the TFR with the charged bilayer/water interface.

(2) The overwhelming fraction of the receptor is oriented with the large head group pointing to the outside (or convex side) of the vesicle.

Transferrin Binding to Reconstituted TFR. In order to test the function of the reconstituted receptor, we studied the binding of fluorescence (FITC)-labeled transferrin as described under Materials and Methods. The results are summarized in Figure 8 for various lipid compositions. In all cases, the fluorescence intensity is plotted as a function of the initial concentration of ligand added to the incubation medium. The fluorescence intensities (Figure 8) of the vesicle suspensions were compared with a standard FITC solution and are thus a direct measure for the amount of ligand bound to the vesicles (cf. Materials and Method). In order to distinguish the specific receptor/ligand binding from the nonspecific binding, the binding curves were simultaneously recorded for both TFR-loaded and TFR-free vesicles. The fraction of receptor binding sites occupied was determined by simultaneous measurement of the receptor concentration. The most important results of the binding studies are as follows:

(1) In the presence of the charged lipid component (cf. case of Figure 8a), the binding curves exhibit a sigmoidal form; that is, significant ligand binding sets in above a threshold concentration. The latter depends on the surface charge (compare panels a and b of Figure 8). In contrast, the binding curve for the case of zwitterionic lipids is of the Langmuir type (Figure 8c).

(2) The nonspecific binding of ligand is much smaller for negatively charged than for noncharged membranes (compare panels a and b with panel c of Figure 8).

(3) Saturation is observed in all cases. However, the maximum fraction of available binding sites which is actually occupied differs remarkably for the three reconstituted systems. It is 18% for the 1:1 DMPC/DMPG mixture, 37% for the 8:2 DMPC/DMPS system, and 65% for the 9:1 DEPE/DEPC mixture.

The ligand binding can be described in terms of a simple kinetic model:

$$[R] + [T] \rightleftharpoons [RT]$$

$$K_d = [R]_s[T]_s/[RT]$$

where [RT] is the concentration of receptor/ligand complexes and $[R]_s$ and $[T]_s$ are the concentrations of the receptor and ligand, respectively, at the membrane surface and K_d is the equilibrium dissociation constant. As follows from the above equation, the differences in the initial slope of the binding curves (of Figure 8a–c) and in the maximum fractions of binding sites occupied could be due (1) to differences in the

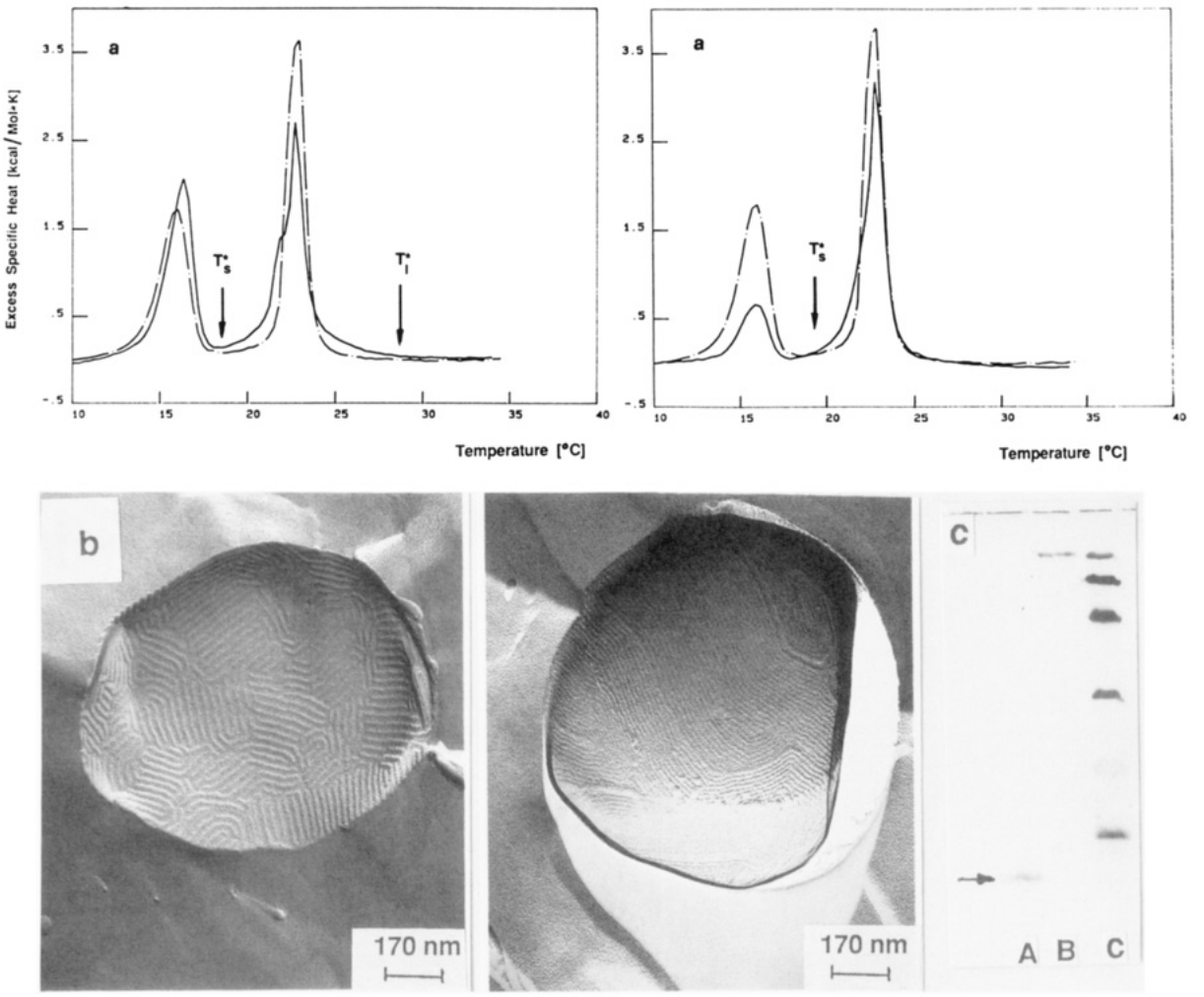

FIGURE 7: (a) Effect of Pronase from *Streptomyces griseus* on calorimetric scanning curves of a 1:1 DMPC/DMPG mixture containing TFR at molar fraction $x_p = 3.22 \times 10^{-4}$. Left, before incubation; right, after incubation with Pronase for 1 h. (b) Freeze–fracture electron micrograph taken before (left) and after (right) incubation with Pronase. Note that Λ texture (wavelength 217 Å) is changed to Λ/2 texture (wavelength 138 Å). (c) SDS gel electrophoresis of a TFR-containing vesicle fraction of a 1:1 DMPC/DMPG mixture before (lane B) and after treatment with Pronase (lane A) and comparison with standard proteins (lane C). The highest band of lane C has a molecular weight of 94K and the lowest 14K. The residual protein fraction after Pronase treatment exhibits a molecular weight of about 10K.

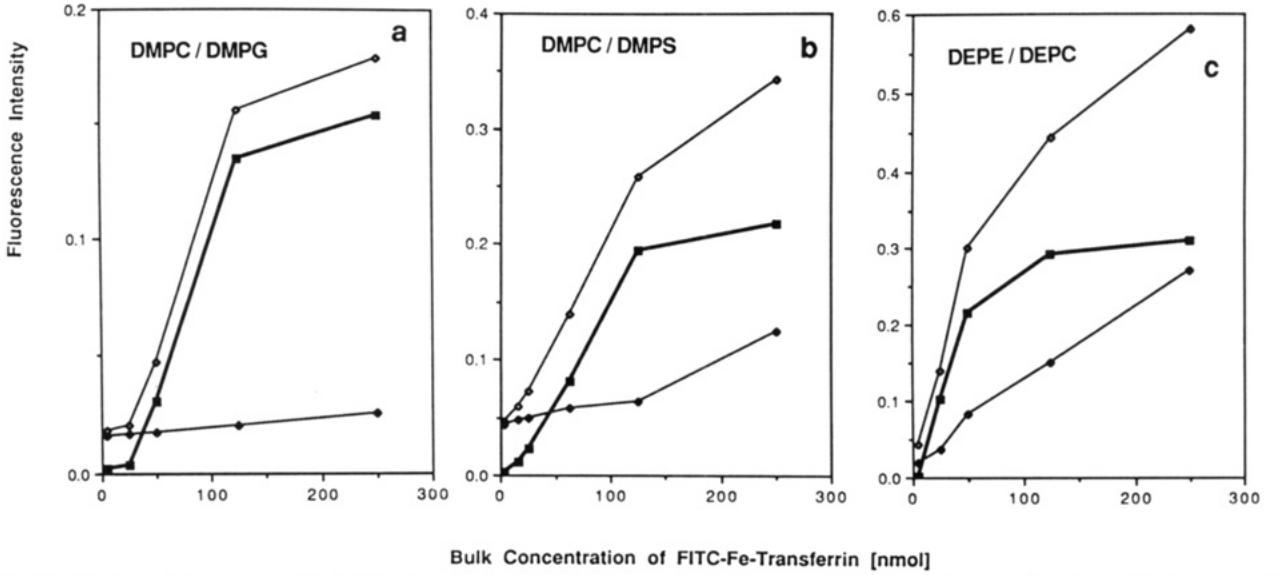

FIGURE 8: Binding of fluorescence labeled Fe–transferrin (FITC–Fe–transferrin) to reconstituted receptor as a function of lipid composition and structure. The fluorescence intensity (which is a quantitative measure for the amount of ligand bound) is plotted as a function of labeled transferrin added to the vesicle suspension for incubation. By subtraction of binding curves obtained for proteoliposomes (◇) and pure vesicle suspensions (♦), the binding curves (■) were corrected for nonspecific binding of ligand to the membrane surface. (a) Binding curves for 1:1 DMPC/DMPG vesicles containing $x_p = 3.7 \times 10^{-4}$ TFR. Maximum fraction of TFR binding sites occupied: 18%. (b) Binding curves for 8:2 DMPC/DMPS vesicles with $x_p = 4.7 \times 10^{-4}$ TFR. Maximum fraction of binding sites occupied: 37%. (c) Binding curves for 9:1 DEPE/DEPC vesicles containing 4.2×10^{-4} TFR. Maximum fraction of binding sites occupied: 65%.

Table I: Maximum Molar Fraction, x_p^{max}, of TFR and Percentage of Initial Concentration Incorporated into Vesicles of Various Lipid Composition[a]

vesicle composition	max TFR content, x_p^{max} ($\times 10^{-4}$)	% incorporated	bilayer fluid thickness (nm)
DMPC	0.5	7	2.3
DEPC	3.4	35	3.1
DEPE/DEPC, 9:1	4.2	52[b]	3.1
DMPC/DMPS, 8:2	4.7	78[c]	2.3
DMPC/DMPG, 9:1	1.9	20	2.3
DMPC/DMPG, 7:3	3.2	42	2.3
DMPC/DMPG, 1:1	3.7	65	2.3

[a] In all cases, the initial protein concentration was $x_p^0 = 5 \times 10^{-4}$ (lipid to protein molar ratio 2000:1). [b] At an initial concentration $x_p^0 = 1 \times 10^{-3}$, the TFR fraction incorporated is 59% (or $x_p^{max} = 9 \times 10^{-4}$). [c] At $x_p^0 = 2 \times 10^{-4}$, the maximum TFR fraction incorporated is 72%; that is, the values given in the table correspond approximately to saturation.

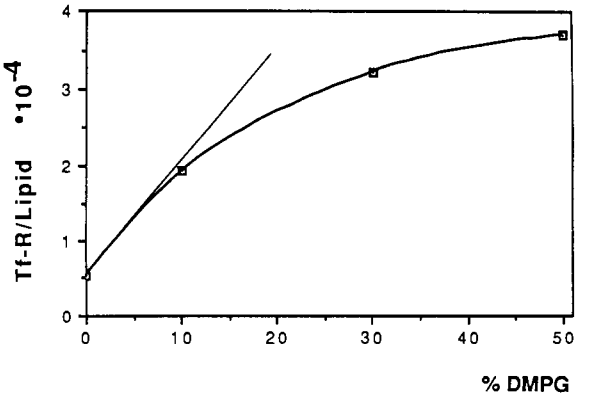

FIGURE 9: Plot of average amount (molar fraction x_p) of transferrin receptor incorporated into DMPC/DMPG mixed vesicles as a function of the charged lipid content. The initial TFR concentration added for the freeze–thaw experiment was $x_p^0 = 5 \times 10^{-4}$.

(surface) concentration of ligands and (2) to differences in the dissociation constant K_d.

We attempted to determine the equilibrium dissociation constant K_d form Scatchard plots. Owing to the small number of points measured, only a rough estimate of K_d was possible. The value obtained, $K_d \approx 10^{-8}$ M, agrees reasonably well with the value of $K_d = 10^{-8}$–10^{-9} M reported by Ward (1987). However, it was not possible to observe differences between the three types of membranes of Figure 8.

The sigmoidal binding curve for charged membranes is most likely the consequence of a ligand depletion layer owing to the negative surface potential. Fe–transferrin has its isoelectric point at pH 5.4 and is thus slightly negatively charged at the pH (=7.8) of the buffer used for the measurement. The concentration of the ligand at the membrane surface is thus smaller than in the bulk, and a threshold concentration is required to overcome repulsion of the ligand. The difference of Figure 8a–c in the maximum fraction of binding sites occupied at saturation is attributed to a change in the dissociation constant (K_d) for the receptor in nonmatched lipid bilayer as will be discussed under Discussion.

Discussion

Saturation Behavior of Protein Incorporation. The present work clearly demonstrates the essential role of elastic and electrostatic forces for lipid/protein self-assembly. This becomes more evident by considering Table I. It summarizes our results concerning the percentage of the initial protein concentration incorporated into the bilayer as a function of the chain length (first three rows) and of the surface charge of the bilayer (last four rows). The initial molar fraction of TFR (with respect to the lipid) added to the vesicle suspension for the freeze–thaw experiment was $x_p^0 = 5 \times 10^{-4}$. However, as follows from the footnote to Table I, these values correspond approximately to the maximum concentrations which can be incorporated. In Figure 9, the maximum TFR concentration, x_p^{max}, incorporated into the DMPC/DMPG mixture (at an initial protein concentration of $x_p^0 = 5 \times 10^{-4}$) is plotted as a function of the charged lipid content of the bilayer. Clearly, saturation behaviour is observed at a TFR concentration of $x_p \approx 4 \times 10^{-4}$ at 50% DMPG. At this concentration, the average distance between the proteins is $l = 28$ nm, which is certainly still small compared to the diameter of the protein head groups so that protein/protein interactions are not responsible for the saturation behavior. Table I suggests the following conclusions:

(1) In the absence of charged lipid, a minimum lipid chain length (or partial matching of the hydrophobic cores of the membrane and the receptor) is required for the incorporation of the receptor. Provided the hydrophobic core of the TFR (ranging from amino acids 62 to 90) would form an α-helix, it would exhibit a length of 4.3 nm. This is still about 1 nm larger than the bilayer thickness of the long-chain lipids (DEPC, DEPE) of 3.1 nm, and a substantial dilatation of the bilayer in the normal direction is required in order to accommodate the protein. If stretching of the lipid chains would be the only mechanism of lipid/protein interaction, one would rather expect a high-temperature shift of the onset of the chain-melting transition according to the mattress model (Mouritsen & Bloom, 1984; Riegler & Möhwald, 1986). This discrepancy would be due to the fact that the interaction of the receptor with the bilayer is also determined largely by the coupling of its head group with the lipid/water interface, as was found in previous studies on the reconstitution of the insulin receptor (Sui et al., 1988) and glycophorin (Rüppel et al., 1982) in DMPC bilayers. Another explanation for the low-temperature shift of T_1 is that the hydrophobic core of the transferrin receptor assumes another conformation than an α-helix. Thus, the total length of a β-sheet configuration of 28 amino acids (distance between two neighbors, 3.47 Å) would be 97 Å. Matching could thus be achieved in the case of the long-chain lipids by 3-fold folding of the hydrophobic domain.

(2) Other evidence for the importance of the hydrophobic (nonelectrostatic) interaction mechanism is provided by our finding (cf. Table I) that the maximum protein concentration, x_p^{max}, incorporated is considerably higher for the 9:1 DEPE/DEPC mixture than for DMPC.

(3) The energy associated with the elastic distortion of the bilayer (due to the mismatch between the hydrophobic cores of the bilayer and the protein) can be overcompensated by the gain of the electrostatic lipid–protein interaction energy.

(4) Considerably more receptor is incorporated into the DMPC vesicles containing DMPS as charged lipid instead of DMPG (compare rows 4–6 of Table I), which shows that the interaction is not purely electrostatic.

Possibility of Elastic Distortion of the Receptor. In the case of the forced incorporation of the receptor into the short-chain lipids by electrostatic forces, either the bilayer or the protein hydrophobic core must be deformed. Evidence for a remarkable conformational change of the TFR in bilayers of lipids with C14 hydrocarbon chains is provided by Figure 8. Only a small fraction of the available receptor binding sites is occupied at saturation: 18% in the case of 1:1 DMPC/DMPG and 37% in the case of 8:2 DMPC/DMPS mixtures. In contrast, the fraction of occupied binding sites is much

higher (65%) if the receptor is contained in the long-chain lipid bilayers. A conformational change by the electrostatic force cannot be excluded, however.

Saturation Behavior of the Interaction of TFR with Charged Lipid. An interesting result of the calorimetric study is that the high-temperature shift ($T_l^* - T_l$) of the liquidus line does not depend on the receptor concentration x_p, in contrast to the behavior for the shift of the solidus line. Such a concentration dependence is indeed predicted by the regular solution theory according to which the excess energy of the lipid/protein interaction is proportional to x_p ($1 - x_p$) [cf. Maksymiw et al. (1987) and Sui et al. (1988)]. The former finding suggests that the receptor interacts with a fixed amount of charged lipid. The stoichiometry of this receptor/lipid complex can be estimated from the initial slope of the plot of the maximum amount of receptor in DMPC/DMPG bilayers as a function of the DMPG content (in Figure 9). This initial slope is a measure for the number of DMPG molecules required by TFR. From Figure 9, one finds $\Delta x_p/\Delta x_{DMPG} \approx n_p/n_{DMPG} \approx 1.3 \times 10^{-3}$ (where n_p and n_{DMPG} are the number of molecules), which would correspond to a DMPG to protein ratio of 1300:1.

Excess Lipid/Protein Interaction Energies. As was shown previously (Maksymiw et al., 1987; Sui et al., 1988), one advantage of calorimetry is that it allows one to obtain quantitative information on the specificity of the lipid/protein interaction in terms of the work associated with the transfer of the proteins from a hypothetical ideal solution to the real membrane (which is a measure for the excess energy of the lipid/protein interaction). However, such information is only obtained if the phase diagram of the pure lipid mixture and its modification by small amounts of protein are measured. Unfortunately, this was not achieved yet. Nevertheless, by assuming that the pure lipid mixture behaves nearly ideally (as is the case for DMPC/DMPG and DMPC/DMPS), the partial excess energy, ΔH_p^{ex}, per mole of protein may be estimated from the shift ($\Delta T_l = T_l^* - T_l$) of the liquidus line according to

$$\Delta H_p^{ex} \approx \frac{\Delta H^0 \Delta T_l x_l}{R T_l^2 x_p}$$

where ΔH^0 is the heat of the $L_\alpha \rightarrow P_{\beta'}$ transition and T_l is the temperature of the liquidus line. For $\Delta H^0 \approx 30$ kJ/mol of lipid, $\Delta T_l \approx 6$ °C, $T_l \approx 300$ K, and $x_p \approx 10^{-4}$, one obtains $\Delta H_p^{ex} \approx 2000$ kJ/mol of protein and $\Delta H_p^{ex} \approx 0.2$ kJ/mol of lipid. These energies are about equal to the corresponding values characterizing the binding of spectrin to DMPC/DMPS vesicles. The binding energy per receptor is thus of the order of 1000 k_BT at 300 K. It should be noted that the above equation holds if the solubility of the protein in the $P_{\beta'}$ phase is negligibly small. ΔH_p^{ex} would be larger at finite protein solubility in the solid state.

Acknowledgments

First, we are most grateful to Th. Bayerl and to the research center of BMW for recording FTIR spectra of vesicle suspensions. Second, we gratefully acknowledge the continuous help of Prof. Riethmüller and his co-workers during the isolation of the TFR.

References

Bach, D. (1984) in *Biomembrane Structure and Function* (Chapman, D., Ed.) Verlag Chemie, Weinheim and Basel.

Cameron, D. G., Casal, H. L., & Mantsch, H. H. (1980) *Biochemistry 19*, 3665–3672.

Jähnig, F. (1978) *J. Chem. Phys. 70*, 3279–3290.

Maksymiw, R., Sui Senfang, Gaub, H., & Sackmann, E. (1987) *Biochemistry 26*, 2983–2990.

McElhaney, R. N. (1986) *Biochim. Biophys. Acta 864*, 361–421.

Minowada, J., Ohnuma, T., & Moore, G. E. (1972) *J. Natl. Cancer Inst. 49*, 891–895.

Mouritsen, O., & Bloom, M. (1984) *Biophys. J. 46*, 141–153.

Nunez, M. T., & Glass, J. (1982) *Biochemistry 21*, 4139–4143.

Riegler, J., & Möhwald, H. (1986) *Biophys. J. 49*, 1111–1118.

Rüppel, D., & Sackmann, E. (1983) *J. Phys. (Paris) 44*, 1025–1034.

Rüppel, D., Kapitza, H.-G., Galla, H.-J., Sixl, F., & Sackmann, E. (1982) *Biochim. Biophys. Acta 692*, 1–17.

Sackmann, E. (1984) *Biological Membranes* (Chapman, D., Ed.) Vol. 5, Chapter 3, pp 106–143 Academic Press, London.

Schneider, C., Newman, R. A., Sutherland, D. R., Asser, U., & Greaves, F. (1982) *J. Biol. Chem. 257*, 10766–10769.

Sperotto, M., & Mouritsen, O. (1988) *Eur. Biophys. J. 16*, 1–10.

Sui Sen-fang, Urumov, T., & Sackmann, E. (1988) *Biochemistry 27*, 7463–7469.

Ward, J. H. (1987) *Invest. Radiol. 22*, 74–83.